CORROSION BEHAVIOR OF 6063 ALUMINUM ALLOY IN ETHYLENE GLYCOL-WATER SOLUTION

A. Qaed Amini Haroooni, H. Eskandari*, M. H. Maddahy, I. Danaee and S. Nikmanesh
* *hadi.nioc@gmail.com*

Abadan Faculty of Petroleum Engineering, Petroleum University of Technology, Abadan, Iran.

Abstract: The electrochemical behavior of 6063 aluminum alloy in ethylene glycol-water mixture was investigated by polarization curves and AC impedance measurements (EIS). The results obtained from polarization curves showed that corrosion rate decreased with increasing ethylene glycol concentration. EIS data showed the decrease in the interface capacitance which caused by adsorption of ethylene glycol at the surface of aluminum alloy. The cathodic current increased with the increase in rotating speeds of solution and the anodic current decreased. The effect of temperature was studied and the corrosion rate was increased with increasing the temperature. In addition, thermodynamic parameters were calculated in different ethylene glycol concentrations.

1. INTRODUCTION

Corrosion, which is an inevitable problem faced by almost all industries, can be considered as one of the worst technical damages of our time [1]. Corrosion is a major problem in the cooling system of an engine block [2]. Aluminum alloys have been used to achieve better corrosion behavior and to replace more traditional materials like stainless steels and copper alloys [3]. Also aluminum alloys are known for their many advantages, such as light density, good mechanical properties, high thermal conductivity, excellent formability, relatively good corrosion resistance, availability and low cost [4-6].

For skin sheet material the emphasis is on achieving a good balance of formability, strength, and a high surface quality after pressing and paint finish. Consequently, the bake hardening 6xxx alloys series are the primary choice for these applications [7]. 6063 aluminum alloy exhibits extremely high resistance to corrosion, highly weldable, and heat treatment add strength to the material when compared to ferrous-based products [8].

The corrosion of aluminum alloys have been studied in aqueous media, in a mixture of desalinated water and in butyl glycol, as well as in water-alcohol media such as automotive engine coolants [2,4,9]. The corrosion of some other alloys such as steels and magnesium in ethylene glycol-water solution have been studied [12-16]. However, limited work was carried out to investigate the aluminum alloy corrosion in coolants such as ethylene glycol-water solution [6,10,11]. Ethylene glycol is widely used as coolant in automotive heat exchangers, mixed with water, in a pH range between 7 and 8, due to its great heat absorption capacity [17]. Currently, the main composition of a conventional coolant is 30-70 V/V% ethylene glycol-water [14].

The objective of this work is to evaluate the corrosion rate of 6063 aluminum alloy in the ethylene glycol-water solution at different concentrations of ethylene glycol, different solution rotating speeds and different temperatures by means of electrochemical measurements, including polarization curves and electrochemical impedance spectroscopy (EIS). In addition, thermodynamic parameters for different concentrations of ethylene glycol were calculated.

2. MATERIALS AND EXPERIMENTAL

Sodium chloride and ethylene glycol used in this work were Merck products of analytical grade and were used without further purifications. Doubly distilled water was used throughout. Aluminum 6063 electrode whose

A. Qaed Amini Haroooni, H. Eskandari, M. H. Maddahy, I. Danaee and S. Nikmanesh

Table 1. Chemical composition of the Aluminum alloy 6063.

Element	Si	Fe	Cu	Mn	Mg	Cr	Zn	Ti	Fe
% wt	0.40	0.35	0.10	0.10	0.60	0.10	0.10	0.10	Balance

chemical composition is shown in table 1 was used as working electrode. Each sample was sealed by polyester resin with an exposed surface area of 1 cm². The exposed areas of the electrodes were mechanically abraded with 400, 800, 1200 and 2000 grades of emery paper, degreased with acetone and rinsed by distilled water before each electrochemical experiment. Metallographic tests were carried out with (Olympus BHZZ-UMA) optical microscope after exposure the samples in ethylene glycol-water solutions.

Corrosion tests were carried out in 100 ppm NaCl aqueous solution with different ethylene glycol concentration. The apparatus for electrochemical investigations consisted of computer controlled AutoLab potentiostat /galvanostat (PGSTAT 302N) corrosion measurement system. Potentiodynamic polarizations were performed at a scan rate of 0.1 mV s^{-1}. Electrochemical measurements were carried out in a conventional three-electrode glass cell. Platinum electrode was used as a counter electrode and a saturated Ag/AgCl as the reference electrode. Signals in EIS measurements were applied in the frequency range from 100 kHz to 1 mHz with a peak-to-peak AC amplitude of 10 mV. In all EIS measurements and polarization experiments, before recording, the working electrode was maintained at its open circuit potential for 15-20 min until a steady state was obtained. Fitting of experimental impedance spectroscopy data to the proposed equivalent circuit was done by AutoLab FRA software.

3. RESULTS AND DISCUSSION

3. 1. Different Concentration

Potentiodynamic polarization curves of aluminum alloy electrode in different concentrations of ethylene glycol solution are shown in Fig. 1. The polarization curves
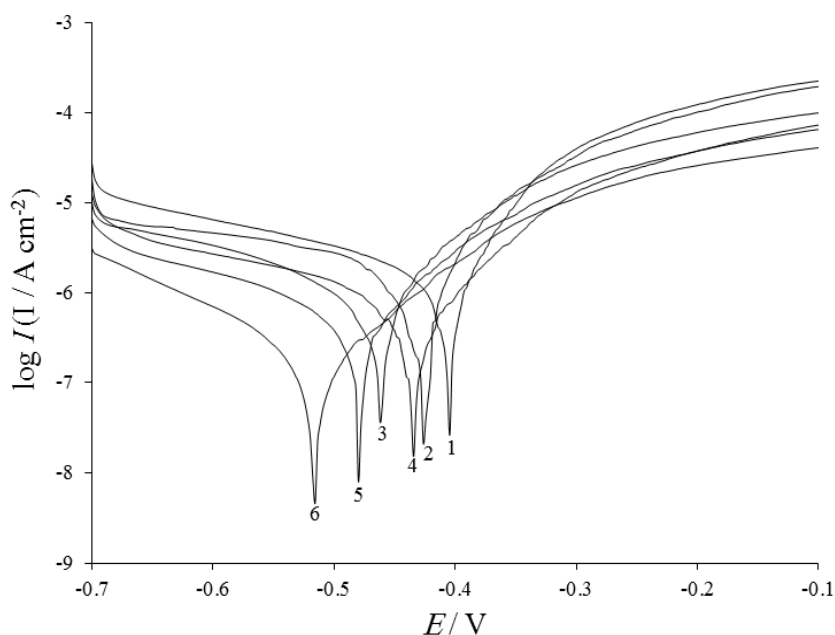

Fig. 1. Polarization curves of aluminum alloy electrode in 100 ppm NaCl and ethylene glycol-water solution with different concentrations of ethylene glycol: 1: 0; 2: 10; 3: 20; 4: 30; 5: 40; 6: 50% V/V ethylene glycol solution.

Table 2. Polarization parameters in the corrosion of Aluminum alloy 6063 in 100 ppm NaCl and ethylene glycol-water solution with different concentrations of ethylene glycol.

Ethylene glycol% V/V	$I_{corr} \times 10^{-6}$ / A.cm^{-2}	β_a	β_c	E_{corr} / V	R_p / Ω	$CR \times 10^{-3}$ mm/year
0	1.149	0.068	-0.162	-0.407	12545	38.62
10	0.961	0.075	-0.221	-0.427	21190	32.98
20	0.765	0.071	-0.149	-0.461	27100	25.86
30	0.532	0.095	-0.196	-0.435	58460	18.14
40	0.305	0.088	-0.140	-0.480	77015	9.024
50	0.133	0.094	-0.122	-0.516	200900	4.510

demonstrate Tafel type behavior of these samples in the active state. Under the condition, the main cathodic reaction is reduction of O_2 [12]. Table 2 gives the values of corrosion parameters for aluminum alloy at different concentrations of ethylene glycol. E_{corr}, I_{corr}, C_R, β_a, β_c and R_p are the corrosion potential, corrosion current density, corrosion rate, anode Tafel constant, cathode Tafel constant and polarization resistance, respectively. The potentiodynamic polarization results were calculated by using Tafel extrapolation method. The Stern-Geary equation (1) was used to calculate the R_p [18].

$$I_{corr} = \frac{\beta_a \beta_c}{2.303(\beta_a + \beta_c)} \left(\frac{1}{R_p}\right) \qquad (1)$$

The open circuit corrosion potentials (OCP) shift to more negative values and a decrease of the corrosion current is observed on the aluminum alloy substrate with the increase of the ethylene glycol concentration. The decrease of the cathodic current is higher than anodic. The results indicate that the corrosion of Al 6063 in an ethylene glycol solution is closely related to the ethylene glycol content of the solution.

In order to get more information about the corrosion phenomena, solution resistance (R_s), charge-transfer resistance (R_{ct}) and double layer capacitance (C_{dl}) of aluminum electrode, impedance measurements was carried out. The Nyquist plot for aluminum sample at different concentrations of ethylene glycol measured at open circuit potential is shown in Fig. 2. The data
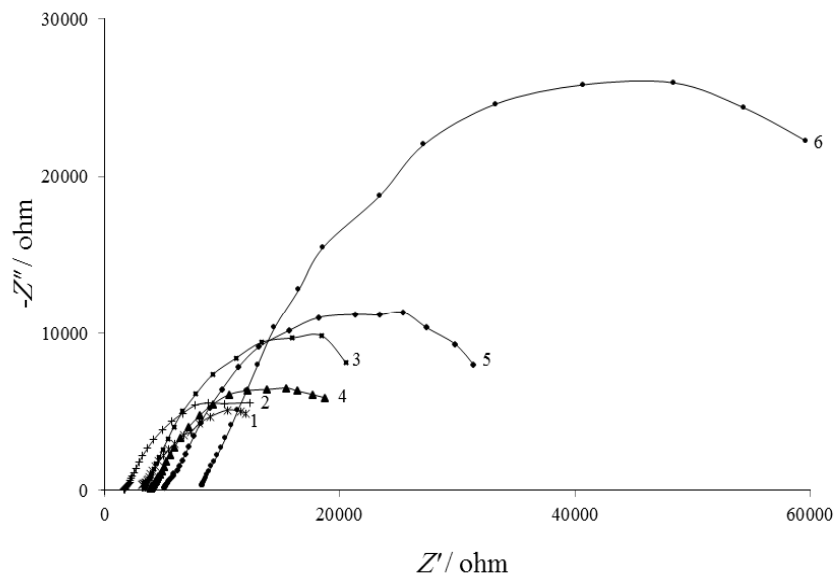
Fig. 2. Nyquist diagrams of aluminum alloy electrode in 100 ppm NaCl and ethylene glycol-water solution with different concentrations of ethylene glycol: 1: 0; 2: 10; 3: 20; 4: 30; 5: 40; 6: 50% V/V ethylene glycol solution.
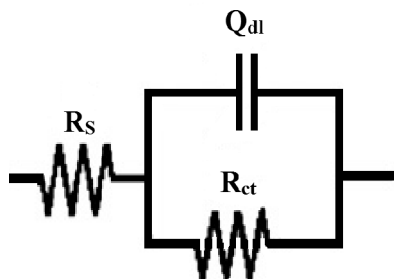
A. Qaed Amini Haroooni, H. Eskandari, M. H. Maddahy, I. Danaee and S. Nikmanesh

Qdl

RS

Rct

Fig. 3. Equivalent circuits compatible with the experimental impedance data in Fig. 2 for corrosion of aluminum alloy electrode in ethylene glycol solution.

reveal that impedance diagram consists of a capacitive loop due to charge transfer resistance and double layer capacitance. The equivalent circuit compatible with the Nyquist diagrams recorded in the presence of ethylene glycol is depicted in Fig. 3. The simplest approach require the theoretical transfer function $Z(\omega)$ to be represented by a parallel combination of a resistance R_{ct} and a capacitance C, both in series with another resistance R_s [19] :

$$Z(\omega) = R_s + \frac{1}{1/R_{ct} + i\omega C_{dl}} \qquad (2)$$

where ω is the frequency in rad/s, $\omega = 2pf$ and f is frequency in Hz. To obtain a satisfactory impedance simulation of aluminum alloy, it is necessary to replace the capacitor (C) with a constant phase element (CPE) Q in the equivalent circuit. The most widely accepted explanation for

the presence of CPE behavior and semicircles on solid electrodes is microscopic roughness, causing an inhomogeneous distribution in the solution resistance as well as in the double layer capacitance [20]. Constant phase element CPE_{dl}, R_s and R_{ct} can be corresponded to double layer capacitance, solution resistance, and charge transfer resistance, respectively. This electrochemical circuit was fitted acceptably on the EIS spectra with mean square error less than 0.05 ($x^2 < 0.05$).

To corroborate the equivalent circuit, the experimental data were fitted to equivalent circuit and the circuit elements were obtained. Table 3 illustrates the equivalent circuit parameters for the impedance spectra of corrosion of aluminum alloy in ethylene glycol solution. From table 3, with increasing ethylene glycol concentration, the solution resistance and charge transfer resistance increases. Pure ethylene glycol has very poor electrical conductivity and is almost an insulator. Therefore, the resistivity of ethylene glycol solution increases with the decrease of the ethylene glycol content. Moreover, the dilution by water may tend to facilitate the hydrolysis of the hydroxyl groups of ethylene glycol, lead to increasing the electrical conductivity as well. As can be seen, the polarization resistance of aluminum alloy in an ethylene glycol solution depends on the solution resistance. As the solution resistance increases with the increase in concentration of ethylene glycol, the polarization resistance also increases [12].

Like most other organic compounds, ethylene glycol should be easily adsorbed on electrode surface [12]. The double layer capacitance is a good indication of the adsorption of ethylene

Table 3. Equivalent circuit parameters in the corrosion of aluminum alloy in 100 ppm NaCl and ethylene glycol-water solution with different concentrations of ethylene glycol.

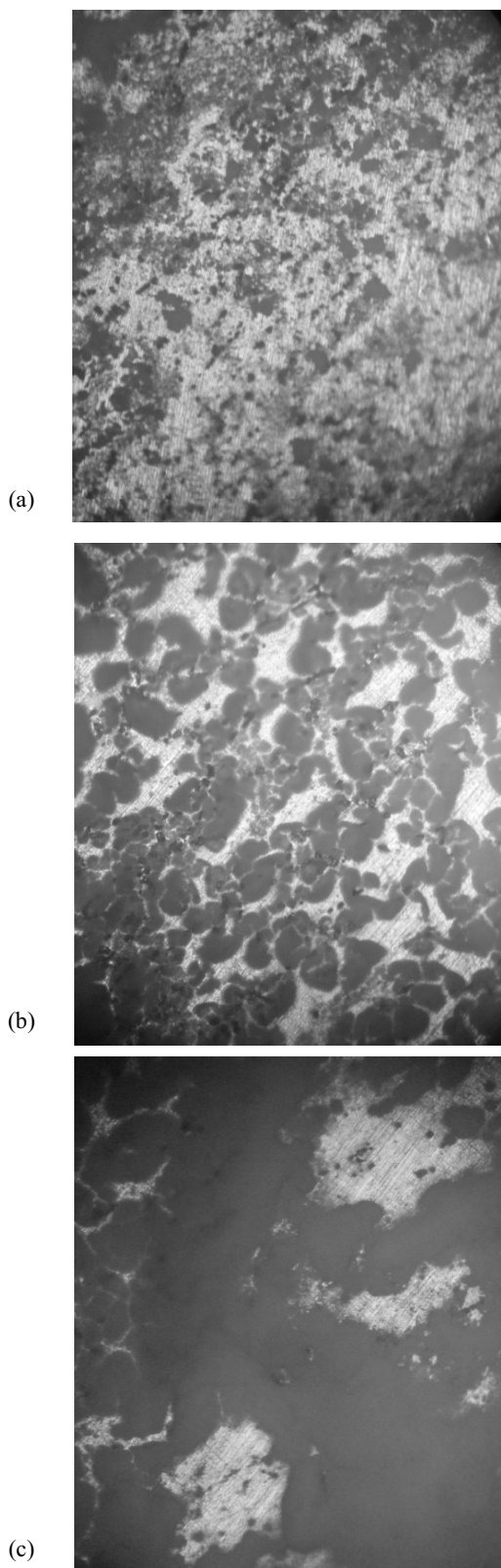| Ethylene glycol% V/V	R_S / $10^3\,\Omega$	R_{ct} / $10^4\,\Omega$	Q_{dl} / 10^{-5} F	n
0	2.191	2.2432	8.3241	0.58
10	1.782	2.1476	3.1199	0.69
20	3.394	2.7419	1.7084	0.76
30	3.885	2.2937	2.9088	0.70
40	5.067	3.6051	1.3505	0.74
50	8.369	7.4325	0.8518	0.76

37

(a)

(b)

(c)

Fig. 4. Surface of aluminum alloy electrode by metallographic microscope in 100 ppm NaCl and 10% - 50 % ethylene glycol-water solution and fresh abraded surface: (a) 10% (b) 30% (c) 50%.

glycol on aluminum alloy surface. Q_{dl} can be easily calculated based on the equivalent circuit of EIS. It appeared that the capacitance tends to decrease as the ethylene glycol concentration increases. This indicates a change at the aluminum alloy/solution interface. A decreasing interface capacitance can be caused by high dielectric water at the interface being replaced by some substance that is larger in molecular size. Ethylene glycol molecule is larger than water, so the adsorption of the former at the surface of aluminum alloy results in a lower Q_{dl}. When the concentration of ethylene glycol increases, more ethylene glycol will be adsorbed on the surface, leading to a lower Q_{dl}. In other words, the aluminum alloy surface is more completely covered by ethylene glycol in a more concentrated ethylene glycol solution, which more effective protect aluminum alloy from the water corrosion attack. This explains the decrease in corrosion rate of aluminum alloy with increasing concentration of ethylene glycol.

Fig. 4 shows the morphologies of the electrode surface in 10, 30, 50% ethylene glycol solution. The metallographic images were recorded after holding the electrode for 24 hours in ethylene glycol solution. It is observed that the sample in 10% ethylene glycol solution has higher corrosion attack (Fig. 4a). On the other hand, in higher ethylene glycol concentration, smoother surface obtains with lower density of pits, and the degree of attack decreases (Fig. 4c).

3. 2. Hydrodynamic Condition

Cathodic and anodic polarization curves of aluminum in 40% ethylene glycol solution at various rotating speeds are presented in Fig. 5. And the orresponding calculations are listed in table 4. It is seen that under static condition, corrosion of the aluminum alloy is mainly controlled by diffusion in cathodic reaction. In addition, corrosion potentials shift to more positive values with increasing the solution rotating speeds 0, 400, 800, 1200 and 1500 rpm. Furthermore, with the increase of solution rotating speed, under the same cathodic polarization potential, the cathodic current densities increase remarkably, while the anodic

Table 4. Polarization parameters in the corrosion of aluminum alloy in ppm NaCl and ethylene glycol-water solution in 40% ethylene glycol solution at various rotating speeds.

Rotation / rpm	$I_{corr} \times 10^{-6}$ /A cm^{-2}	β_a	β_c	E_{corr} / V	R_p / Ω	$CR \times 10^{-3}$ mm year^{-1}
0	0.305	0.088	-0.140	-0.480	77015	7.69
400	0.431	0.082	-0.151	-0.447	53590	11.46
800	0.632	0.074	-0.160	-0.411	34820	21.47
1200	1.042	0.110	-0.225	-0.378	30830	35.31
1500	1.518	0.111	-0.243	-0.345	21825	51.50

current densities decrease. The dissolved oxygen diffuses toward the aluminum alloy electrode, and the oxygen reduction reaction generates hydroxide ions that use by the oxidation of aluminum to form aluminum oxide, resulting in the positive shift of corrosion potential. The increase in solution rotation would accelerate the diffusion of oxygen toward the electrode surface for cathodic reduction reaction. Consequently, the oxidation of aluminum enhances due to the substantial supplement of oxidant, resulting in formation of aluminum oxide film on electrode surface and thus the decrease of the anodic

dissolution current of aluminum electrode. Therefore, with increasing the electrode rotation speed, the cathodic current density increases while the anodic current density decreases. Proliferate of noises in cathodic and anodic polarization curves with increasing the solution rotating speed is another notable point due to high speed and unsettlement of solution.

3. 3. Different Temperatures

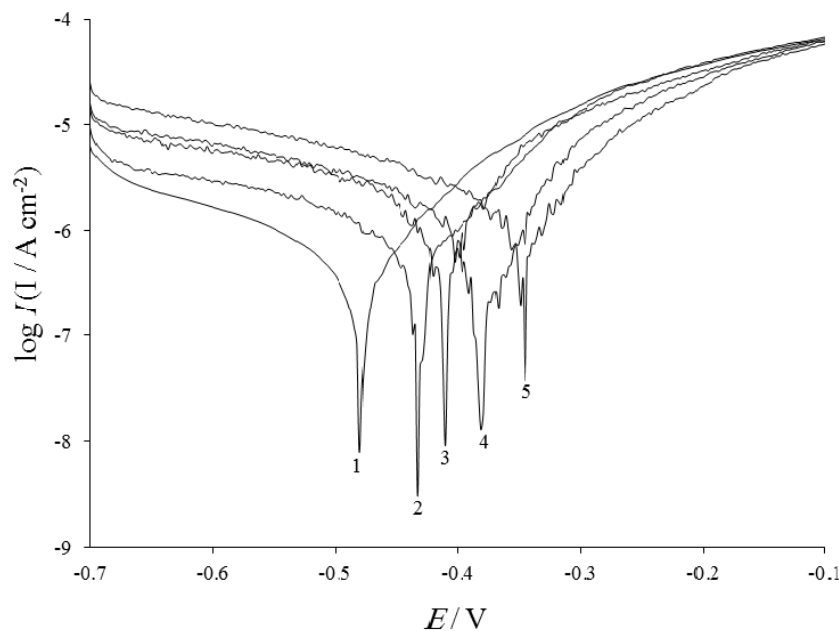Current-potential characteristics resulting from cathodic and anodic polarization curves of

Fig. 5. Polarization curves of aluminum alloy electrode in 100 ppm NaCl and 40% ethylene glycol-water solution with different solution rotating speeds: 1: 0; 2: 400; 3: 800; 4: 1200; 5: 1500 rpm.

Table 5. Polarization parameters in the corrosion of aluminum alloy in 100 ppm NaCl and ethylene glycol-water solution in 30% ethylene glycol solution at various temperature.

Temp / °C	$I_{corr} \times 10^{-6}$ / A cm^{-2}	β_a	β_c	E_{corr} / V	R_p / Ω	$CR \times 10^{-2}$ mm year^{-1}
R.T	0.532	0.110	-0.296	-0.435	65540	1.81
30	1.184	0.082	-0.289	-0.419	23600	3.98
50	1.414	0.090	-0.302	-0.450	21287	4.80
70	2.719	0.078	-0.235	-0.448	9395	9.23
90	9.999	0.038	-0.333	-0.479	1483	33.3

aluminum in 30% ethylene glycol solution at various temperature are shown in Fig. 6 and Tafel calculations are listed in table 5. It is seen that, with the increase of solution temperature, under the same cathodic and anodic polarization potential, the cathodic and anodic current densities increase remarkably. The increasing solution temperature would accelerate both the cathodic reduction and anodic oxidation reaction [21]. This can be explained by the decrease in the strength of the adsorption process at elevated temperature and would suggest a physical adsorption mode.

The effect of temperature on the corrosion reaction is very complex, because many changes occur on the metal surface. The change of the corrosion current at selected concentrations of the ethylene glycol was studied in 100×10^{-6} ppm NaCl solution at three temperatures (298, 318 and 338 K) and the results are listed in table 6. In the presence of the ethylene glycol, the corrosion current of aluminum alloy decreases at any given temperature as the ethylene glycol concentration increases. In contrast, at constant ethylene glycol concentration, the corrosion current increases with rising as the temperature. To calculate
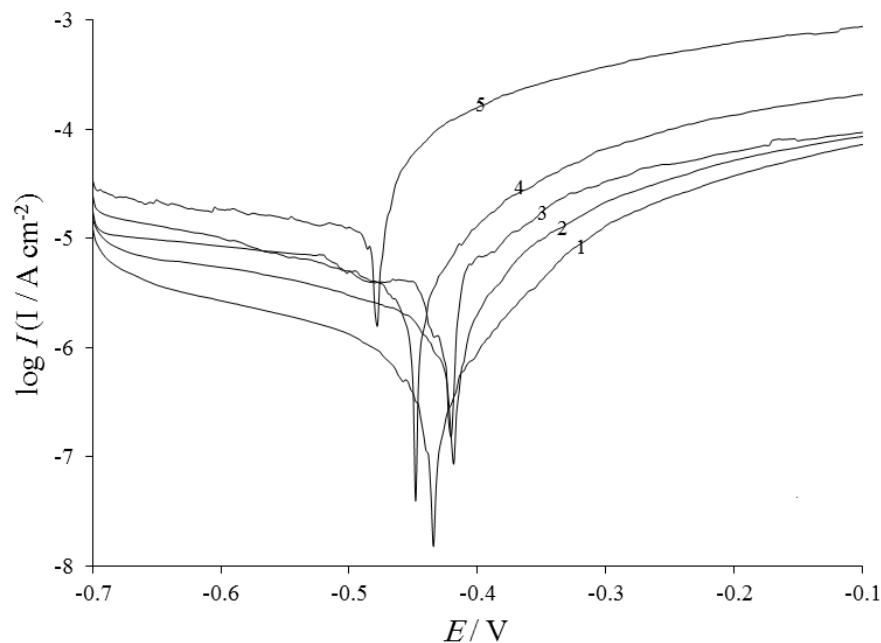

Fig. 6. Polarization curves of aluminum alloy electrode in 100 ppm NaCl and 30% ethylene glycol-water solution with different temperature: 1: R.T; 2: 30; 3: 50; 4: 70; 5: 90 °C.

Table 6. Polarization parameters in the corrosion of 6063 aluminum alloy in 100 ppm NaCl with ethylene glycol at different temperature.

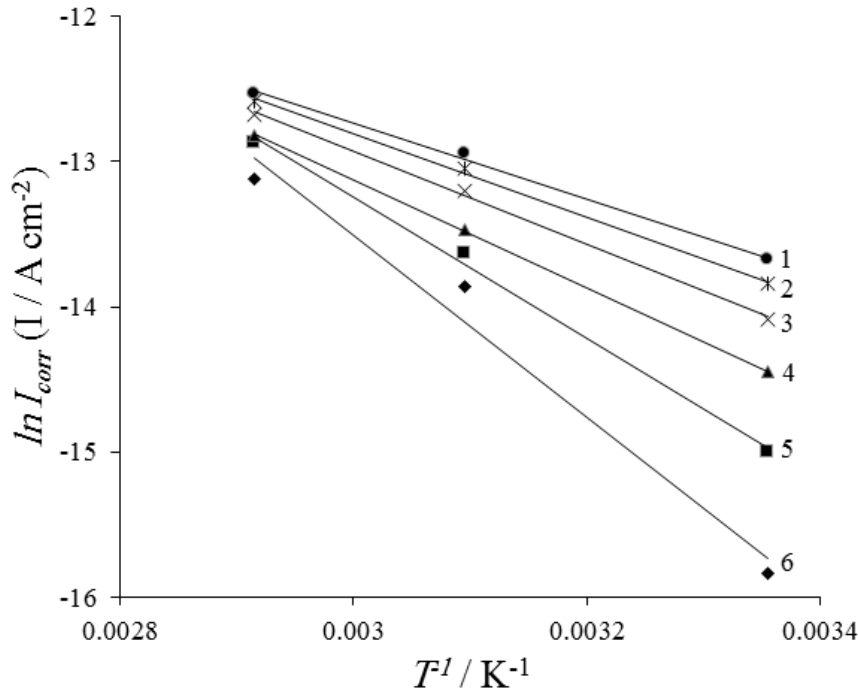| Ethylene glycol% V/V	$I_{corr} \times 10^{-6}$ (298 K) / A cm^{-2}	$I_{corr} \times 10^{-6}$ (323 K) / A cm^{-2}	$I_{corr} \times 10^{-6}$ (343 K) / A cm^{-2}
0	1.149	2.388	3.624
10	0.972	2.153	3.426
20	0.765	1.846	3.121
30	0.532	1.414	2.719
40	0.305	1.194	2.562
50	0.133	0.956	2.012

Fig. 7. Typical Arrhenius plots of lnI$_{corr}$ vs. T^{-1} for aluminum alloy in 100 ppm NaCl at different concentrations of ethylene glycol: 1: 50; 2: 40; 3: 30; 4: 20; 5: 10; 6: 0% V/V

activation thermodynamic parameters of the corrosion process, Arrhenius Eq. (3) and transition state Eq. (4) are used [22, 23]:

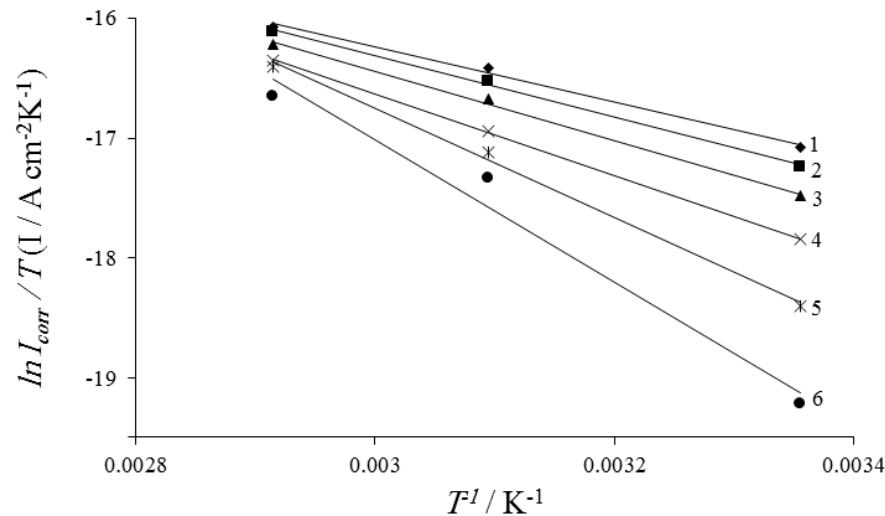$$I_{corr} = Ka \exp\left(\frac{-Ea}{RT}\right) \qquad (3)$$

$$I_{corr} = \left(\frac{RT}{Nh}\right)\exp\left(\frac{\Delta S_a}{R}\right)\exp\left(\frac{-\Delta H_a}{RT}\right) \qquad (4)$$

where E_a is the apparent activation energy of corrosion, R is the universal gas constant, K_a is the Arrhenius pre-exponential factor, h is the Plank's constant, N is the Avogadro's number, ΔS_a is the change in entropy of activation and ΔH_a is the change in enthalpy of activation.

Values of apparent activation energy of corrosion (E_a) for aluminum alloy with the absence and presence of various concentrations of ethylene glycol were determined from the slope of lnIcorr vs. 1/T plots (Fig. 7) and are shown in table 7. This reveals that the corrosion

Table 7. Values of activation parameters Ea, ΔHa and ΔSa for 6063 aluminum alloy in 100 ppm NaCl with different concentration of ethylene glycol.

Ethylene glycol% V/V	E_a / kJ mol^{-1}	K_a / A cm^{-2}	ΔH_a / kJ mol^{-1}	ΔS_a / kJ mol^{-1}K^{-1}	$RT=E_a - \Delta H_a$ / kJ mol^{-1}
0	21.82	0.0078	19.09	-256.07	2.73
10	23.92	0.0154	21.27	-250.08	2.64
20	26.68	0.0375	24.00	-242.93	2.68
30	30.86	0.1364	28.27	-231.79	2.59
40	40.46	3.8658	37.87	-204.01	2.59
50	52.16	203.16	49.33	-171.84	2.84

Fig. 8. Typical Arrhenius plots of ln(I_{corr}T^{-1})vs. T^{-1} for aluminum alloy in 100 ppm NaCl at different concentrations of ethylene glycol: 1: 50; 2: 40; 3: 30; 4: 20; 5: 10; 6: 0% V/V

process is slower in the presence of ethylene glycol. In addition, plots of ln(I_{corr}/T) against 1/T (Fig. 8) gives a straight line with a slope of (-ΔH_a / R) and an intercept of (lnR/N_h + ΔS_a / R) from which the values of ΔH_a and ΔS_a are calculated and are listed in Table 8. This result verifies the known thermodynamic reaction between the E_a and ΔH_a as shown in Table 8 [22]:

$$\Delta H_a = E_a - RT \qquad (5)$$

The positive values of ΔH_a mean that the dissolution reaction is an endothermic process.

One can notice that Ea and ΔH_a are of the same order. On the other hand, ΔS_a increases more positively with increasing ethylene glycol concentrations (Table 7) and their values are negative in different concentrations of ethylene glycol. This reflects the formation of an ordered stable layer of the ethylene glycol on the aluminum alloy surface [24]. The negative values of entropies imply that a decrease in disordering takes place on going from reactants to the adsorbed system [25].

4. CONCLUSION

The corrosion of aluminum alloy 6063 was

studied through electrochemical methods in ethylene glycol-water mixture with different concentrations, rotating speeds and temperatures. The results revealed that the corrosion current decreased and corrosion potential shifted to more negative potential with increasing ethylene glycol concentration. A decreasing interface capacitance can be caused by adsorption of the former at the surface of the aluminum alloy due to larger molecular size of ethylene glycol molecules.

The results of different rotating speeds indicated that with the increasing solution rotating speeds, i.e., the enhanced hydrodynamic condition, the oxygen diffusion accelerated. The reaction on the cathodic reduction increased and led to increasing of current density in cathodic region, while aluminum alloy was oxidized to form a layer of oxide film to decrease the anodic current density. Corrosion potential shifted to more positive potential with increasing rotating speed of ethylene glycol-water solution.

With increasing the temperature, corrosion current increased and thermodynamic adsorption parameters showed that ethylene glycol adsorbed on surface by an exothermic, spontaneous process.

REFERENCES

1. Stansbury, E. E., Buchanan, R. A., "Fundamentals of electrochemical corrosion"., USA, ASM international, 2000, 2-4.

2. Xu, L. Y., and Cheng, Y. F., "Effect of fluid hydrodynamics on flow-assisted corrosion of aluminum alloy in ethylene glycol–water solution studied by a microelectrode technique". J. Corrosion Science. 2009, 10, 2330-2335.

3. Niu, L., and Cheng, Y. F., "Synergistic effects of fluid flow and sand particles on erosion–corrosion of aluminum in ethylene glycol–water solutions". J. Wear., 2008, 265-3, 367-374.

4. Zhang, G. A., Xu, L. Y., and Cheng, Y. F., "Mechanistic aspects of electrochemical corrosion of aluminum alloy in ethylene glycol–water solution". J. Electrochimica Acta., 2008, 53-28, 8245-8252.

5. Abiola, O. K., and Otaigbe, J. O. E., "Effect of common water contaminants on the corrosion of aluminium alloys in ethylene glycol–water solution". J. Corrosion Science., 2008, 50-1, 242-247.

6. Krishnamurthy, K., and Venkatesh, J., "Assessment of surface roughness and material removal rate on machining of TIB2 reinforced Aluminum 6063 composites: A Taguchi's approach". J. International Journal of Scientific and Research Publications., 2013, 3-1.

7. Miller, W. S., Zhuang, L., Bottema, J., Wittebrood, A. J., De Smet, P., Haszler, A., and Vieregge, A., "Recent development in aluminium alloys for the automotive industry". J. Materials Science and Engineering., 2000, 280-1, 37-49.

8. Sherwood, P. W., "Performance of aluminum in refineries". J. Anti-Corrosion Methods and Materials., 1959, 6-12, 375-378.

9. Leong, K. Y., Saidur, R., Kazi, S. N., and Mamun, A. H., "Performance investigation of an automotive car radiator operated with nanofluid-based coolants (nanofluid as a coolant in a radiator)." Applied Thermal Engineering., 2010, 30-17, 2685-2692.

10. Zhang, G. A., Xu, L. Y., and Cheng, Y. F., "Investigation of erosion–corrosion of 3003 aluminum alloy in ethylene glycol–water solution by impingement jet system." J. Corrosion Science., 2009, 51-2, 283-290.

11. Zaharieva, J., Milanova, M., Mitov, M., Lutov, L., Manev, S., and Todorovsky, D., "Corrosion of aluminium and aluminium alloy in ethylene glycol–water mixtures". J. Journal of Alloys and Compounds, 2009, 470-1, 397-403.

12. Danaee, I., Niknejad Khomami, M., and Attar, A. A., "Corrosion behavior of AISI 4130 steel alloy in ethylene glycol–water mixture in presence of molybdate". J. Materials Chemistry and Physics, 135-2, 658-667.

13. Danaee, I., Niknejad Khomami, M., and Attar, A. A., "Corrosion of AISI 4130 Steel Alloy under Hydrodynamic Condition in Ethylene Glycol+ Water+ NO_2- Solution". J. Journal of Materials Science & Technology, 2013, 29-1, 89-96.

14. Song, G., and StJohn, D., "Corrosion behaviour of magnesium in ethylene glycol". J. Corrosion Science., 2004, 46-6, 1381-1399.

15. Fekry, A. M., and Fatayerji, M. Z., "Electrochemical corrosion behavior of AZ91D alloy in ethylene glycol". J. Electrochimica Acta., 2009, 54-26, 6522-6528.

16. Samiento-Bustos, E., Rodriguez, J. G., Uruchurtu, J., Dominguez-Patiño, G., and Salinas-Bravo, V. M., "Effect of inorganic inhibitors on the corrosion behavior of 1018 carbon steel in the LiBr+ ethylene glycol+ H_2O mixture". J. Corrosion Science., 2008, 50-8, 2296-2303.

17. Samiento-Bustos, E., González-Rodriguez, J. G., Uruchurtu, J., and Salinas-Bravo, V. M., "Corrosion behavior of iron-based alloys in the LiBr+ ethylene glycol+ H_2O mixture". J. Corrosion Science., 2009, 51-5, 1107-1114.

18. Macdonald, D. D., and Urquidi-Macdonald, M., "Application of Kramers-Kronig Transforms in the Analysis of Electrochemical Systems I. Polarization Resistance". J. Journal of the Electrochemical Society., 1985, 132-10, 2316-2319.

19. Jafarian, M., Gobal, F., Danaee, I., Biabani, R., and Mahjani, M. G., "Electrochemical studies of the pitting corrosion of tin in citric acid solution containing Cl-". J. Electrochimica Acta., 2008, 53-13, 4528-4536.

20. Danaee, I., and Noori, S., "Kinetics of the hydrogen evolution reaction on NiMn graphite modified electrode". J. International Journal of Hydrogen Energy., 2011, 36-19, 12102-12111.

21. Antunes, R. A., de Almeida Machado, C. A.V., and Correa, O. V., "Influence of testing temperature on the corrosion behavior of API 5L X70 pipeline." Proceedings of the Unified 22nd International Congress of Mechanical Engineering. Conf., Ribeirão Preto, SP, Brazil, 2013,.

22. El Bribri, A., Tabyaoui, M., Tabyaoui, B., El Attari, H., and Bentiss, F., "The use of 'Euphorbia falcata' extract as eco-friendly corrosion inhibitor of carbon steel in hydrochloric acid solution". J. Materials Chemistry and Physics., 2013, 141-1, 240-247.

23. Morad, M. S., and El-Dean, A. M., "2, 2′-dithiobis (3-cyano-4, 6-dimethylpyridine): a new class of acid corrosion inhibitors for mild steel". J. Corrosion science., 2006, 48-11, 3398-3412.

24. Ghasemi, O., Danaee, I., Rashed, G. R., RashvandAvei, M., and Maddahy, M. H., "The inhibition effect of synthesized 4-hydroxybenzaldehyde-1, 3propandiamine on the corrosion of mild steel in 1 M HCl". J. Journal of materials engineering and performance., 2013, 22-4, 1054-1063.

25. Herrag, L., Hammouti, B., Elkadiri, S., Aouniti, A., Jama, C., Vezin, H., and Bentiss, F., "Adsorption properties and inhibition of mild steel corrosion in hydrochloric solution by some newly synthesized diamine derivatives: experimental and theoretical investigations". J. Corrosion Science., 2010, 52-9, 3042-3051.